

Unsteady RANS Simulation of High Reynolds Number Trailing Edge Flow

D. Ang¹, L. Chen² and J. Tu¹

¹School of Aerospace, Mechanical & Manufacturing Engineering
Royal Melbourne Institute of Technology, VIC, 3083 AUSTRALIA

²Defence Science & Technology Organisation
Aeronautical and Maritime Research Laboratory, VIC, 3001 AUSTRALIA

Abstract

Unsteady vortex shedding at a trailing edge may cause pressure fluctuations and strong tonal noise which can have important consequences to the performance of marine and aeronautical type lifting surfaces. This paper presents data from unsteady RANS simulation of high Reynolds number trailing edge flow. It aims to identify and quantify dominant features of the trailing edge flow field over a two-dimensional hydrofoil at Reynolds numbers of chord (Re) from 1.4×10^6 to 8.0×10^6 . The foil section is a NACA0015 profile with a trailing edge cut at 0.2% chord from the trailing edge.

It is found that the onset of vortex shedding occurs at a bluntness parameter $h/\delta^* \geq 0.28$ and $Re_h \geq 1.9 \times 10^4$, where h is the characteristic length scale of the trailing edge bluntness, δ^* is the boundary layer displacement thickness and Re_h is the Reynolds number based on h .

Introduction

The flow of an incompressible viscous fluid over a submerged lifting surface at high Reynolds numbers induces a variety of fluid phenomena. Laminar boundary layers form at the leading edge and depending on the viscosity of the flow, may quickly transition into turbulence which completely envelops both sides of the lifting surface near the trailing edge. Turbulent boundary layers near the trailing edge generate broadband scattering noise as well as surface pressure fluctuations which tend to excite structural vibration and fatigue [1]. Furthermore, separation of the turbulent boundary layer at the trailing edge can cause sustained shedding of vortices into the wake and generate tonal noise. An accurate prediction of trailing edge flows is therefore crucial to estimate the associated noise.

The onset of vortex shedding at the trailing edge is closely related to the characteristics of the boundary layer flow near the trailing edge and its bluntness, h/δ^* [1]. Thus significant changes in Reynolds number and slight modifications to trailing edge geometry may lead to fundamental changes in the trailing edge boundary layer flow. This, in turn, affects the near wake flow and modifies the shedding of vorticity into the wake [2].

This type of turbulent flow over hydrofoils or aerofoils is of particular interest to designers of propellers, control surfaces and lifting devices seeking quiet high performance components. Examination of the two-dimensional flows over hydrofoils can give insight into how the trailing edge geometry influences performance measures such as lift, drag and pressure loss, as well as the magnitude and nature of damaging structural vibration and the generated noise from surface pressure fluctuations. Numerical simulation provides an avenue for potentially accurate prediction of this damaging phenomenon. However, despite the rapid increase of computer power, analysis of such complex flows by Direct Numerical Simulation (DNS) and the alternative technique, Large-Eddy Simulation (LES), remains

computationally expensive. Thus, the modelling of high Reynolds number flows continues to be based on the solution of the Reynolds-averaged Navier-Stokes (RANS) equations despite the claims of experts that the noise generating eddies over a wide range of length scales cannot be adequately represented by RANS equations [3].

This paper presents the development of a numerical prediction method using the commercial computational fluid dynamics (CFD) code of FLUENT based on RANS equations to determine the extent to which RANS modelling can predict trailing edge flow and tonal noise. The following will thus be a close examination of the trailing-edge and near wake flow over a hydrofoil at high Reynolds numbers to verify the relationship between the trailing edge parameter h/δ^* , and the occurrence of vortex shedding. The validation of the turbulence model used for high Reynolds number hydrofoil flows has been reported by Mulvany et. al. [4]. The time-averaged results of displacement thickness are compared to semi-empirical data on flat plate boundary layer growth. The computed results are then used to obtain the unsteady turbulent flow field around the trailing edge and the time history of surface pressure fluctuations and velocity changes in the wake. The frequency spectra of the pressure fluctuations can thus be calculated and the resultant Strouhal numbers compared with published data from Blake [1].

The case under study is a two-dimensional hydrofoil with a NACA0015 section and chord length of 540mm. This symmetrical profile represents a generic section shape used on submerged control surfaces for submarines and ships. Limitations on current manufacturing equipment make it impossible to produce a perfectly sharp trailing edge. To accommodate this, the hydrofoil is 'cut' at 0.2% chord from the trailing edge resulting in a blunt edge with a vertical height of just over 2mm. The hydrofoil is aligned at zero degrees to the incident uniform stream of 2, 5, 7, and 11.5m/s which correspond to Reynolds numbers of chord based on freestream velocity U_{ref} of 1.4, 3.5, 4.9, and 8.0×10^6 respectively.

Figure 1 shows the trailing edge geometry under investigation and a close-up on the blunt edge. Stations A, B, C, D and E refer to measurement stations of pressure fluctuations on the upper surface of the hydrofoil. They are located 100mm from the trailing edge $x_A=438.92$, 70mm from the trailing edge $x_B=468.92$, 40mm from the trailing edge $x_C=498.92$, 0.95 chord lengths from the leading edge $x_D=513$ and at the trailing edge $x_E=538.92$ respectively. Station F refers to the horizontal line offset 0.5mm above the chord line which runs from the blunt edge, through the wake and to the rear end of the control region. The time-history of the vertical velocity along this line is recorded to give an assessment of the fluctuating vorticity in the wake. The value of displacement thickness, δ^* used to calculate the bluntness parameter, h/δ^* is calculated from the boundary layer velocity profile at a distance of $0.2Y_f$ as defined in Blake for the edge geometry under investigation [1].

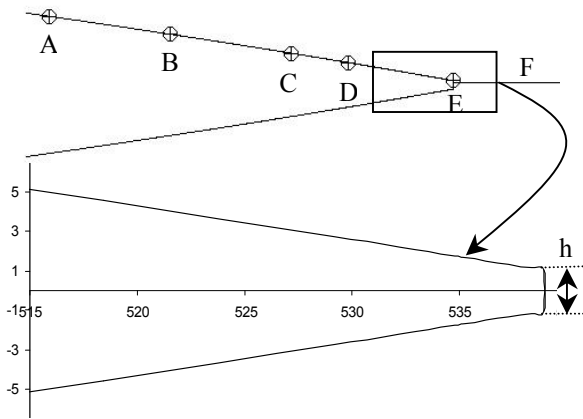


Figure 1. Hydrofoil geometry and measurement stations located at $x_A=438.92$, $x_B=468.92$, $x_C=498.92$, $x_D=513$, $x_E=538.92$ and F which is a horizontal line running from the blunt edge and through the wake.

Computational Methodology

The solution of the flow field is achieved using the commercial CFD code FLUENT. The unsteady segregated solver is utilised with 2nd order implicit approximation of the governing equations. Pressure-velocity coupling is achieved using the SIMPLE method. The time advancement is determined by the fixed time step size Δt , which is initially set to a sufficiently small value to achieve convergence of the residuals after 25 iterations. FLUENT provides a range of Reynolds-averaged turbulence models. Based on published results, the realizable k- ϵ model with enhanced wall treatment was chosen as it provides superior performance over the other available models under adverse pressure gradients, separation and recirculation [4].

The computational domain contains the full hydrofoil section within a rectangular control region. The control region which is 1.5 chord lengths in front, above and below the leading edge of the hydrofoil and 3.5 chord lengths behind the trailing edge is sufficiently distanced from the hydrofoil's surface as to have negligible effect on the solution. 'Velocity inlet' boundary conditions are specified at the front, upper and lower boundaries of the control region to allow the definition and variation of flow upstream of the hydrofoil. The 'outflow' boundary condition is used at the outlet and no-slip wall boundary conditions are defined for the surfaces of the hydrofoil.

The computational grid is meshed with quadrilateral cells using a structured multi-block method. The control region is thus divided into fifty, four-sided map meshed faces. Strong control over the density and distribution of cells is achieved through independent meshing of each block using edge mesh stretching schemes. Special care is given to the near-wall region with appropriate clustering to resolve the viscous sublayer of the boundary layer. As required by the enhanced wall treatment, the wall-adjacent cells should be of the order of $y^+ = 1$ and have at least 10 cells within the viscous sublayer [4]. To reduce the computational cost, the mesh is stretched in the near-wall regions and increase in area away from the wall. Furthermore, transitional cells are utilised to reduce the fine mesh close to the hydrofoil to achieve a coarse mesh in the outer region. The wake region is meshed with a greater density of cells. The near wake and trailing edge region is refined further through hanging node grid adaption. Attention is required in critical regions of the flow where it is important that the mesh is mostly orthogonal to the flow, has minimal skewness and acceptable aspect ratios.

A steady state solution is first obtained to set the initial conditions for the time-dependent solution. 10,000 iterations are

sufficient for the lift and drag coefficients to converge. To simulate the unsteady flow field, the hydrofoil is given an initial perturbation of small vertical velocity for 100 time steps at a very small time interval of 5×10^{-5} seconds. After this initial perturbation, the hydrofoil is again subjected to uniform flow to allow the perturbation to convect out of the computation domain before data sampling is activated to obtain the time-averaged result.

Simulation Results

The grid independence test was conducted on five meshes for $Re=8.0 \times 10^6$. Table 1 details the maximum node y^+ and drag coefficients of each mesh. Mesh 3, 4 and 5 predict almost identical drag coefficients, suggesting that grid independence is achieved. Mesh 4 is selected considering that the maximum y^+ is approximately one as required [4].

Mesh	No. of Cells	Maximum y^+	$C_d (x10^{-3})$
1	69,844	7.993	5.786
2	111,394	5.481	5.674
3	178,852	3.373	5.178
4	279,216	1.005	5.161
5	329,968	1.017	5.159

Table 1. Maximum wall y^+ and drag coefficients achieved for grid independence analysis.

The overall flow field around the hydrofoil is well behaved as expected for a symmetrical section of moderate thickness. In the viscous region close to the surface of the hydrofoil, laminar boundary layers develop at the leading edge, thicken and quickly transition to turbulence. The transition to turbulence is characterised by a large increase in wall shear stress which occurs at approximately 0.01 chord lengths from the leading edge for all Reynolds numbers investigated in this study. Thus, the upper and lower surface of the hydrofoil are nearly completely enveloped in turbulent boundary layer flow, which separates at the salient edge and interacts to form a turbulent wake downstream.

Due to the convergence of the pressure and suction surface of the hydrofoil aft of the point of maximum thickness, the flow close to the surface decelerates, causing a gradient of increasing static pressure. This is particularly evident in the region of the trailing edge as illustrated in Figure 2. This adverse pressure gradient causes a greater thickening of the boundary layer compared to that expected over a flat plate.

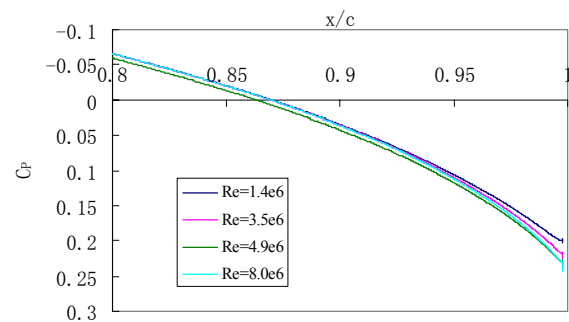


Figure 2. Mean surface pressure coefficient distribution over the pressure surface near the trailing edge for all Reynolds numbers under investigation.

Figure 3 shows the displacement thickness of the boundary layer as it develops over the trailing edge. In comparison, the displacement thickness for a fully turbulent flat plate in a uniform stream of 11.5m/s is only slightly thinner than that for the equivalent hydrofoil case at 80% chord but differs significantly as the trailing edge is approached. This rapid thickening of the boundary layer at the trailing edge influences the Reynolds number at which vortex shedding occurs. Several trends are observed with the increase in Reynolds number. Clearly, there is a general thinning of the boundary layer over the hydrofoil. This is due to the diminishing viscous effects of the flow which also results in a reduction of skin friction drag. Close examination of Figure 2 and the base pressure coefficient measured at the centre of the blunt edge, Figure 4, shows that the pressure at the trailing edge increases with Reynolds number which offsets the pressure drag and further reduces the overall drag coefficient.

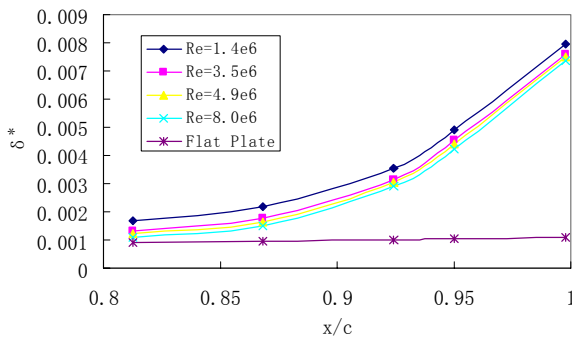


Figure 3. Displacement thickness of the boundary layer as it develops over the trailing edge of the hydrofoil compared to that of a flat plate for $U_{ref}=11.5\text{m/s}$.

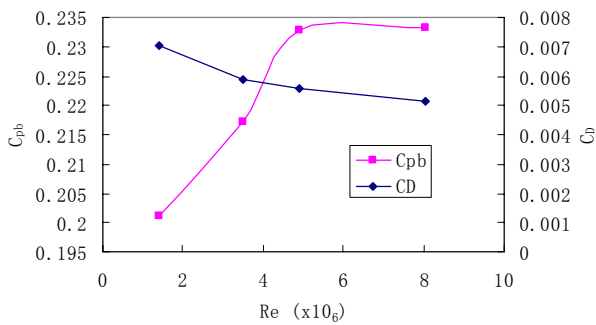


Figure 4. Variation of drag coefficient, C_D and base pressure coefficient C_{pb} , with increasing Reynolds number.

For examination of the unsteady flow characteristics, the instantaneous vorticity magnitude contours in the region of the near wake for the Reynolds numbers under investigation are shown in Figure 5. Figure 5a and 5b clearly show that for $Re=1.4 \times 10^6$ and $Re=3.5 \times 10^6$, vortex shedding does not occur and the separated flow past the trailing edge combines to form two standing eddies of opposite sign but equal magnitude in the near wake. On the other hand, the vorticity fields in Figure 5c and 5d show evidence of vortex shedding in the wake for $Re=4.9 \times 10^6$ and $Re=8.0 \times 10^6$, which decays in strength with increasing distance from the trailing edge.

The time history of vertical velocity fluctuations through the wake is plotted in Figure 6. In response to the initial perturbation, the oscillating flow of the wake is damped and clearly subsides with time for the case of $Re=1.4 \times 10^6$ and 3.5×10^6 , whereas the sustained shedding of vorticity is observed for $Re=4.9 \times 10^6$ and $Re=8.0 \times 10^6$. This result will be further validated using LES simulation.

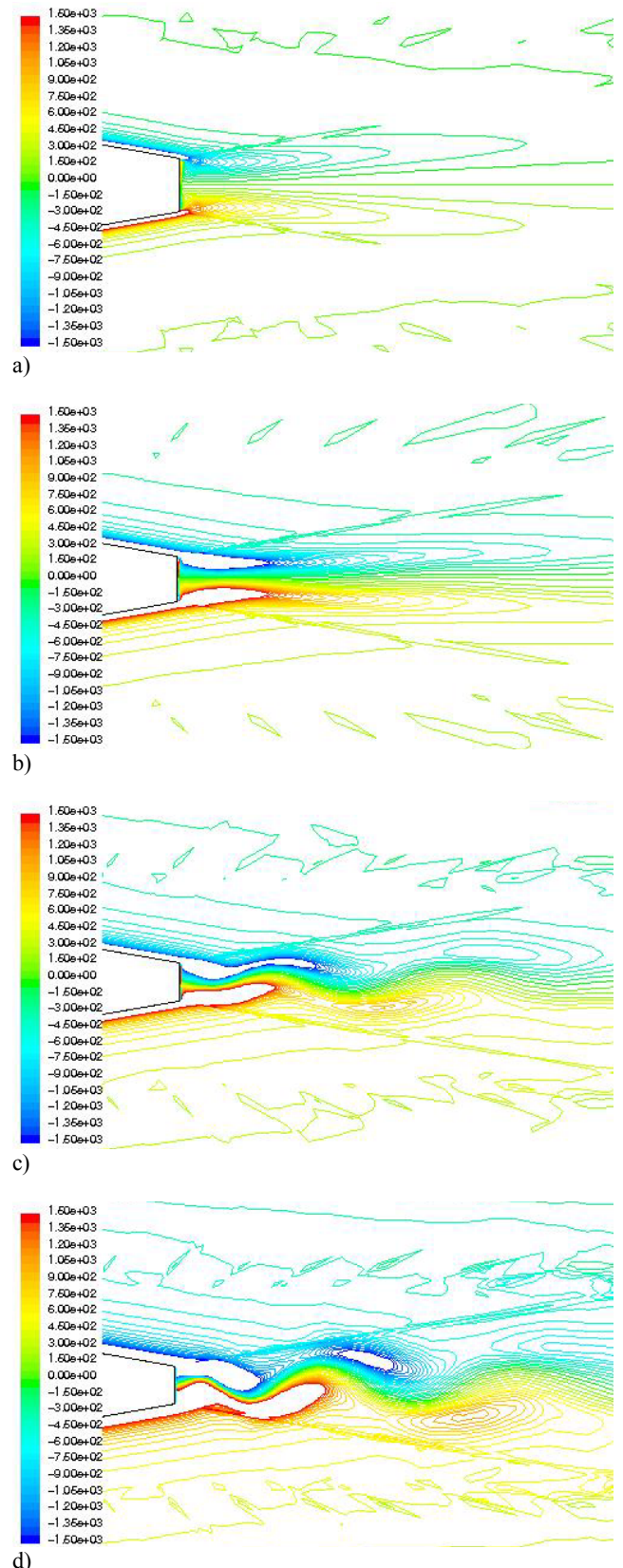


Figure 5. Instantaneous vorticity fields computed from RANS for: a) $Re=1.4 \times 10^6$, b) $Re=3.5 \times 10^6$, c) $Re=4.9 \times 10^6$ and d) $Re=8.0 \times 10^6$ (contour levels from $-1500 \rightarrow 1500$ of vorticity magnitude).

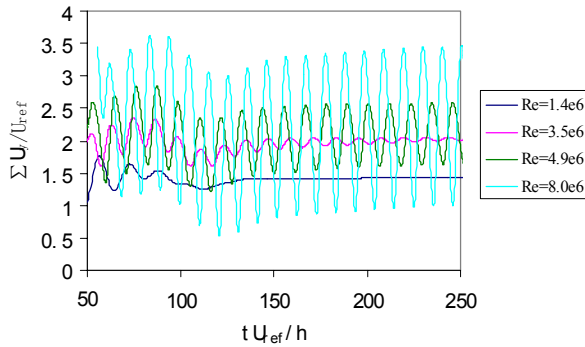


Figure 6. Time history of the vertical velocity along the horizontal line defined as station F in Figure 1, for $Re=1.4 \times 10^6$, 3.5×10^6 , 4.9×10^6 and 8.0×10^6 .

The pressure differentials induced by vortex shedding across the surface of the hydrofoil were observed to be a maximum at the trailing edge. Figure 7 shows the corresponding frequency spectrum of the surface pressure fluctuation at “station E” obtained through Fast Fourier Transformation (FFT). The largest peak in the frequency spectrum corresponds to the vortex shedding Strouhal number. The discontinuities in the broadband spectral noise may be attributed to the limited number of pressure data used for the spectral analysis.

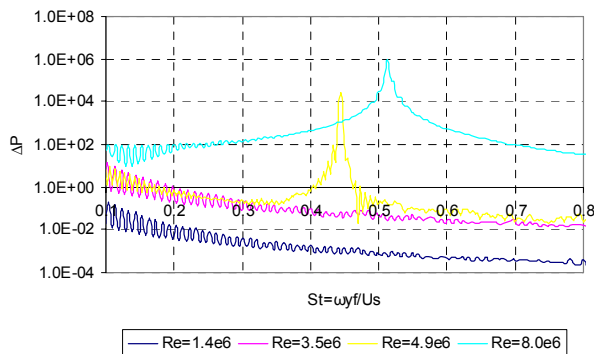


Figure 7. Spectrum analysis of surface pressure fluctuations at the trailing edge, Station E, for $Re=1.4 \times 10^6$, 4.9×10^6 and 8.0×10^6 .

Table 2 contains a summary of the displacement thickness at the trailing edge, the bluntness parameter, h/δ^* and the observed tonal frequency generated at each Reynolds number calculated with reference to the blunt edge height. Figure 8 shows the variation of time-averaged wake dimensions L_f/h and Y_f/h with increasing Reynolds number.

Re_h ($\times 10^4$)	δ^* (mm)	h/δ^*	Vortex Shedding	f_s (Hz)	St
0.538	7.916	0.263	No	-	-
1.345	7.554	0.275	No	-	-
1.883	7.445	0.279	Yes	298	0.444
3.094	7.301	0.285	Yes	527	0.513

Table 2. Summary of vortex shedding strouhal number and bluntness parameters.

Thus the onset of vortex shedding occurs at $h/\delta^* \geq 0.28$ which is comparably close to Blake’s prediction of $h/\delta^* \geq 0.3$. This corresponds to a Re_h of 1.8×10^4 and wake dimension Y_f/h of 0.70. Compared to the published results in Blake [1] for a similar blunt edge geometry, the onset of vortex shedding occurs at Re_h of 0.4×10^4 and the corresponding value of Y_f/h and St are 1.0 and 0.85 respectively. Note, that the experimental results were based

on a significantly larger bluntness parameter, h/δ^* of 5.88 which may be the reason for the differences in the compared results. Also, the rapid thickening of the boundary layer at the trailing edge decreases h/δ^* and thus delays the onset of vortex shedding until higher Re_h values are achieved.

Several similarities of the wake dimensions are observed compared to the wakes of cylinders just before and after the onset of vortex shedding. As Reynolds number of the flow increases, the length of the formation region L_f/h initially increases and then decreases upon the onset of vortex shedding. Furthermore, the intensity of the generated tone increases, characterised by a larger peak in the frequency spectrum [1].

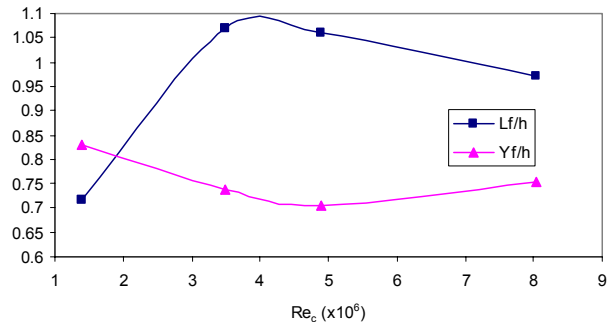


Figure 8. Variation of wake dimensions L_f/h and Y_f/h with increasing Reynolds number.

Conclusions

The dynamic trailing edge and near wake flow have been successfully simulated using unsteady RANS turbulence models. It is found that the onset of vortex shedding is strongly related to Re_h and the characteristics of the trailing edge. For a given trailing edge geometry, the increase of Re_h thins the boundary layer at the trailing edge which increases the likelihood of vortex shedding.

Overall, the RANS equations appear to reasonably predict the onset of vortex shedding. This occurs at $h/\delta^* \geq 0.28$ which is comparably close to results in Blake [1]. However the observed Strouhal numbers do not correlate well with published experimental results for a similar blunt edge geometry. This may be attributed to the inability of the RANS model to accurately obtain the time-averaged wake dimensions of the unsteady wake, which are used as scaling factors for the calculation of the Strouhal number.

References

- [1] Blake, W. K., *Mechanics of Flow-Induced Sound and Vibration*, Vols. 1 and 2, Academic, London, 1986.
- [2] Bourgoyne, D. A., Hamel, J. M., Ceccio, S. L. & Dowling, D. R., Time-averaged flow over a hydrofoil at high Reynolds number, *J. Fluid Mech.*, **496**, 2003, 365-404.
- [3] Wang, M. & Moin, P., Computation of Trailing-Edge Flow and Noise Using Large-Eddy Simulation, *AIAA Journal*, **38**, 2000, 2201-2209.
- [4] Mulvany, N., Tu, J.Y., Chen, L., Anderson, B., Assessment of Two-Equation Turbulence Modelling for High Speed Reynolds Number Hydrofoil Flow, *Int. J. Numer. Methods Fluids*, **45**, 2004, 275-299.